

Stability differences and conversion mechanism between nanotubes and scrolls

Savas Berber and David Tománek

Department of Physics and Astronomy, Michigan State University, East Lansing, Michigan 48824-2320, USA

(Received 13 February 2004; published 21 June 2004)

Using total energy and structure optimization calculations, we investigate the relative stability and the conversion mechanism between multiwall carbon nanotubes and graphitic scrolls. We suggest that axial segments of a nanotube and a scroll may coexist within the same tubular nanostructure, separated by a dislocation region. A scroll may convert to the more stable nanotube by concerted bond-rearrangement rather than bond breaking. We postulate the zipperlike conversion to proceed very efficiently due to the unusually low associated activation barrier.

DOI: 10.1103/PhysRevB.69.233404

PACS number(s): 81.07.De, 81.05.Zx

Combining atomic-scale perfection with a nanometer-size diameter and millimeter-size length, carbon nanotubes^{1,2} are considered important pioneers of nanotechnology. These narrow graphitic cylinders with tunable electronic properties³⁻⁵ are being considered as functional building blocks of nanoscale devices. An important challenge in nanotechnology will be to connect these substructures to more complex systems using bond rearrangements as an atomic-scale counterpart of welding.

When observed in the High Resolution Transmission Electron Microscopy (HRTEM) images of carbon arc-discharge deposits,¹ the symmetric, evenly spaced line patterns have been interpreted as images of coaxial, nested graphitic tubules. Alternatively, the same images have been attributed to graphitic scroll structures.⁶ Distinguishing between the two structures appears to be impossible based on electron micrographs alone.⁷ HRTEM observations suggest presence of radially⁸ and even axially⁹ coexisting scroll and multiwall segments within the same tubular structure. The latter observation introduces two intriguing problems, namely the detailed morphology within the coexistence region, and the possibility of a scroll-to-tube conversion.

Here we present the first study of the relative stability and the microscopic inter-conversion mechanism between axially coexisting multiwall nanotubes and scrolls. We show that scroll segments, consisting of rolled-up graphene sheets, may coexist with nested tube segments within a contiguous tubular nanostructure. We propose a concerted bond rearrangement mechanism that avoids bond breaking and results in an axial zipperlike motion of the scroll/tube dislocation. The energy cost associated with creating this dislocation is low enough to form scroll/nanotube junctions at temperatures occurring during nanotube synthesis. The activation barrier for the subsequent scroll-to-nanotube transformation is sufficiently low to enable conversion even at room temperature.

Available experimental data suggest that nested tubes and scrolls only coexist axially in structures with very many walls.⁹ Due to their large size and lack of periodicity, these systems pose an awesome computational challenge. The most suitable formalism to describe accurately the relative energies of large, defect-free tube or scroll segments is based on continuum elasticity theory.^{10,11} This approach proved to be accurate in comparison to *ab initio* total energy calculations for selected single-wall nanotubes,^{10,11} and also offers

intuitive insight into the origin of structural changes. The major limitation of the continuum approach is its inability to deal with atomic defects. For accurate structural and energy information about defective structures, including coexisting scrolls and tubes, we combine the continuum approach with atomistic calculations.

The continuum energy functional, which describes defect-free single-wall and multiwall tubes as well as scrolls, contains the strain energy ΔE_s , the interwall interaction ΔE_{iw} , and an energy term ΔE_e associated with the creation of an exposed edge in scrolls. In order to avoid energy terms associated with tube ends, we only consider infinitely long structures. We compare structures with the same total area $A=WL$, where W is the nominal width and L the length of a rectangular graphene layer taken as a reference. This reference system has no unsaturated edges and the same number of atoms as the sp^2 bonded tubular structures.

The strain energy, caused by deforming a graphene monolayer into a cylinder of local radius R , depicted in Fig. 1(a), is given by $\Delta E_s = \epsilon_{cyl}L/R$, where L is the length of the tubular structure. *Ab initio* calculations for single-wall tubes suggest a value of $\epsilon_{cyl}=4.43$ eV, related to the flexural rigidity of a graphene monolayer.¹⁰ Since strain energy favors geometries with minimum curvature, it must be compensated by other energy terms to stabilize tubular structures. In multiwalled systems, this compensating energy is provided by the attractive inter-layer interaction $\Delta E_{iw} = \epsilon_i A_c$, where A_c is the contact area between sp^2 bonded layers.¹² Since the interwall separation of $\Delta R=0.34$ nm appears to be common to multiwall tubes, scrolls and graphite, we use $\epsilon_i=2.48$ eV/nm², based on the interlayer interaction in bulk graphite. In scrolls, we also need to consider the energy penalty associated with creating an exposed edge, given by $\Delta E_e = \epsilon_e L$. We use $\epsilon_e=21$ eV/nm as an average value for graphite,¹³ thus ignoring the small difference between a zigzag and an armchair edge.

In tubular systems, all these energy terms are proportional to the tube length L . For a multiwall nanotube, the energy per unit length is given by

$$\frac{E_{tube}}{L} = \sum_n \left(\frac{\epsilon_{cyl}}{R_{in} + (n-1)\Delta R} \right) - \epsilon_i [W - \pi(R_{in} + R_{out})], \quad (1)$$

with the summation extending over the individual walls.

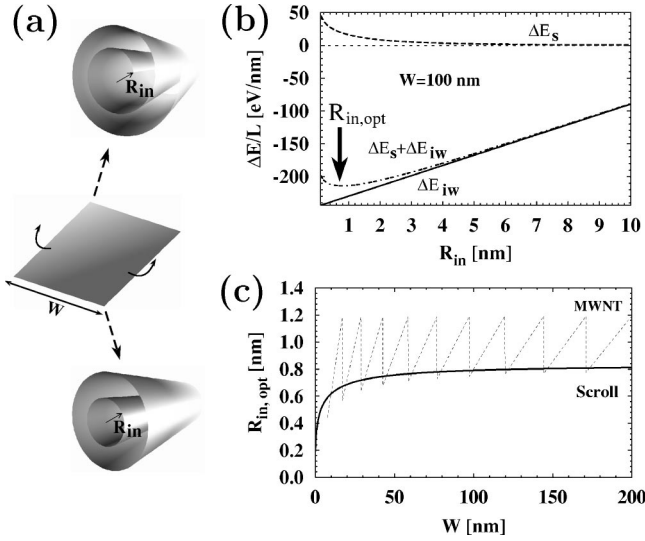


FIG. 1. (a) Schematic of the transformation from a planar graphene strip of width W to a scroll and a multiwall nanotube. (b) Dependence of the strain energy ΔE_s and the interwall interaction energy ΔE_{iw} on the interior radius R_{in} of a scroll, formed from a $W=100$ nm wide reference strip. The optimum value of $R_{in,opt}$ results from a compromise between reducing strain and maximizing the interlayer attraction. The dashed zero line indicates the energy of the reference structure. (c) Dependence of the optimum interior radius of a scroll (solid line) and a multiwall nanotube (dashed line) on W . Abrupt changes of $R_{in,opt}$ occur in multi-wall structures, when the optimum number of walls changes.

The corresponding expression for a scroll is obtained by replacing the summation by an integral over the deformed layer, augmented by the energy penalty associated with the exposed edge. We use the angle θ in cylindrical coordinates as a convenient integration variable, yielding

$$\frac{\Delta E_s}{L} = \frac{\epsilon_{cyl}}{2\pi} \int_0^{\theta_{max}} \frac{1}{R(\theta)} d\theta, \quad (2)$$

where $R(\theta) = R_{in} + \theta \Delta R / 2\pi$ is the local radius of curvature, and θ_{max} is determined by R_{in} and the initial width W of the reference layer. Combining this strain energy with the other remaining terms leads to a scroll energy per unit length of

$$\frac{E_{scr}}{L} = \frac{\epsilon_{cyl}}{\Delta R} \ln\left(\frac{R_{out}}{R_{in}}\right) - \epsilon_i [W - \pi(R_{in} + R_{out})] + 2\epsilon_e. \quad (3)$$

The last term is the exposed edge penalty, which does not depend on the width W of the reference layer and becomes negligibly small in comparison to the other terms in multi-wall systems. We note that providing W and R_{in} defines uniquely the structure of the system, including the number of walls.

Since the edge energy does not depend on R_{in} , we only need to consider the strain and the interwall energy when optimizing the scroll structure. The dependence of $\Delta E_s/L$ and $\Delta E_{iw}/L$ on the interior radius is shown in Fig. 1(b) for a fixed width $W=100$ nm of the reference layer. We find that the strain energy ΔE_s decreases with increasing interior radius and asymptotically approaches the zero value of the

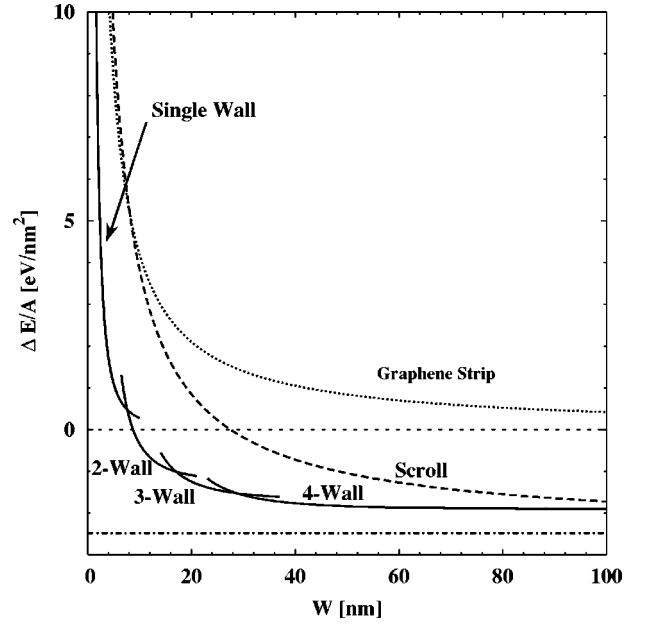


FIG. 2. Total energy of multiwall tubes and scrolls with respect to a reference graphene strip of the same length and width W . Tubular structures with one and more walls are energetically preferred due to the absence of exposed edges, especially at large values of W , and approach the stability of bulk graphite. Also the higher stability of multiwall tubes over scrolls results from the absence of exposed edges.

planar reference layer. Increasing R_{in} for a fixed value of W , on the other hand, reduces the number of walls and the attractive inter-wall interaction ΔE_{iw} . The sum of these energies, given by the dashed-dotted line in Fig. 1(b), shows a shallow minimum at the optimum value $R_{in,opt}$ of the interior radius. This fact suggests that small deviations from the equilibrium structure cost very little energy and are within the reach of thermal processes.

In Fig. 1(c), we display the dependence of the optimum interior radius on the reference layer width. In scrolls, represented by the solid line, we find that the optimum interior radius increases monotonically with increasing W and slowly approaches $R_{in,opt} \lesssim 0.9$ nm. The saturation behavior of $R_{in,opt}(W)$, seen in Fig. 1(c), results from the fact that an increase of R_{in} beyond a certain value should have little effect on the strain energy, but would significantly reduce the interwall attraction. The above considerations apply only to equilibrium structures formed in absence of boundary conditions, such as catalyst particles or other templates. Thus, an important confirmation of our picture is the observation that many multiwall structures, formed in free space and in absence of catalysts, have large interior radii close to 0.9 nm. Multiwall tubes follow a similar general trend as scrolls with the exception that the optimum number of walls changes abruptly. Such changes occur whenever the width exceeds certain threshold values W_n , where the strain energy sacrifice associated with more walls of smaller radius is compensated by the increased interwall attraction.

Our energy results for optimized multiwall tubes and scrolls are summarized in Fig. 2. All energies are given per area and referred to an infinite graphene layer, shown by the

dashed line at $\Delta E/A=0$. Bulk graphite, the most stable carbon allotrope, is stabilized by the interlayer interaction with respect to the monolayer and represented by the horizontal dashed-dotted line. The energy of a graphene strip, given by the dotted line, is dominated by the exposed edge penalty, when the width W is small. At very small values of W , cylindrical deformation of the strip is energetically prohibitive. Only for wide enough strips, the interwall attraction may outweigh the strain energy, stabilizing the scroll with respect to a planar structure. According to Fig. 2, the narrowest scroll may form when $W \approx 8.4$ nm. For $W \geq 28$ nm, the stabilizing interwall interaction outweighs even the exposed edge energy and the scroll becomes more stable than the infinite reference layer.

Due to the absence of the exposed edge energy penalty, we always can find tubes with one or multiple walls that are more stable than a scroll, as seen in Fig. 2. Since the relative importance of the exposed edge decreases with increasing W , we find the energy difference between multiwall tubes and scrolls to decrease rapidly with increasing number of walls. In very large multiwall structures, we postulate that scroll and nanotube segments may even coexist. We also identify a stepwise conversion mechanism of scroll segments into more stable multiwall nanotube segments.

A possible way to connect a scroll with a nanotube within a contiguous structure is shown schematically in Fig. 3(a). In this origami-style counterpart of the system, the tube segment is separated from the scroll by a dislocation region, formed by axially cutting and reconnecting adjacent layers. Obviously, the local morphology, depicted in Fig. 3(b), can be extended to any number of walls. By axially displacing the dislocation in the direction of the arrow in Fig. 3(b), a scroll can be gradually converted to a multiwall nanotube.

To globally optimize the infinite structure containing a nanotube/scroll junction, depicted in Fig. 3(c), we separate the total energy into two parts. Far away from the junction, the energy and equilibrium structure of the infinite scroll and multiwall nanotube segments is determined by continuum elasticity theory, as described above. As seen in Fig. 1(c), optimized structures with very many walls have nearly identical innermost and outermost radii and can be joined smoothly with the exception of the dislocation region. To optimize the atomic structure in the finite region near the junction, shown in Fig. 3(d), we make use of an electronic structure calculation, based on the parametrized linear combination of atomic orbitals (LCAO) formalism,¹⁴ which has been used to accurately describe rebonding and growth at the edge of multiwall nanotubes.¹⁵

Junctions of multiwall nanotubes with scrolls, depicted in Figs. 3(a) and 3(c), contain the type of dislocations, represented in Figs. 3(b) and 3(d), in each layer. In a multilayer system, the total strain is minimized, when the dislocation line is shortest. In a tubular system, the preferential arrangement would correspond to radially stacked dislocations. In systems with very many walls, where scroll/nanotube coexistence has been observed,⁹ the average local curvature is small. The optimum geometry and strain energy in a radial stack of tube dislocations is represented well by a periodic stack of defects connecting graphitic layers, illustrated in Fig. 3(b), with the atomic structure of the unit cell depicted

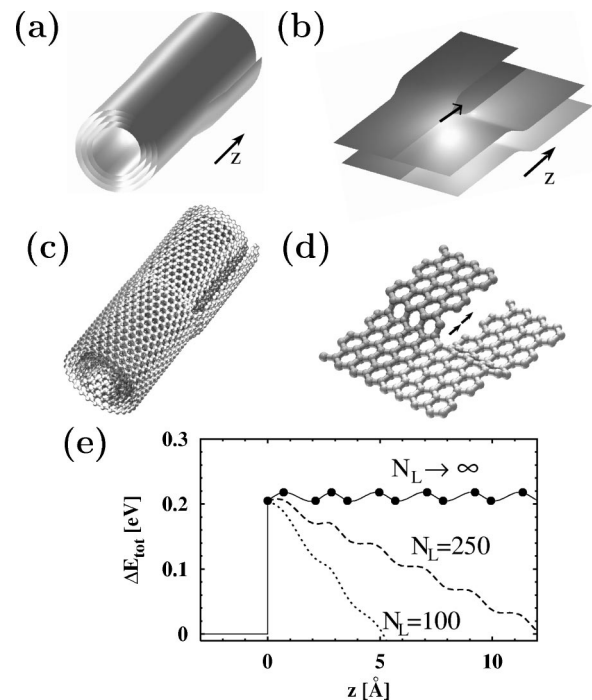


FIG. 3. (a) A hybrid multiwall structure with scroll and multiwall tube segments, shown from the tube end. (b) Schematic structure of two adjacent layers close to the dislocation core near the nanotube/scroll junction. The axial dislocation motion is indicated by the arrow. (c) Equilibrium structure of three innermost walls within an optimized multiwall system. (d) Atomic structure within the unit cell of an infinite periodic stack of dislocations. The zipperlike propagation of the dislocation along the tube axis z is indicated by the arrow. (e) Total energy change ΔE_{tot} per graphitic layer during the zipperlike scroll-to-tube conversion within the hybrid structure. $z > 0$ denotes the axial position of the dislocation. $z < 0$ corresponds to the multiwall tube segment.

in Fig. 3(d). Such an infinite periodic stack of dislocations is formed by rigidly connecting layers without introducing dangling bonds, in analogy to graphitic “foam.”¹⁶ Prior to relaxation, each layer contains two fourfold coordinated, sp^3 bonded atoms in the defect region. Our results suggest that formation of this defect requires an energy investment of only ≈ 0.2 eV per layer in a structure consisting of infinitely many infinitely large layers.¹⁷ Thus, nanotube/scroll hybrids may form under synthesis conditions, which typically involve high temperatures close to 1000 K.

The zipperlike transformation is achieved by displacing the dislocation region in the direction of the arrows in Figs. 3(b) and 3(d). Displacing the dislocation core by one unit cell of the sp^2 structure yields a morphologically identical system with the same energy, provided the structure is periodic in all directions. Only when the number of layers N_L is finite and the energy of the exposed edges in the scroll segment can not be neglected, does the total energy per layer change by $\partial(E_{tot}(z)/N_L)/\partial z = 2\epsilon_e/N_L = (42 \text{ eV/nm})/N_L$ due to the axial dislocation motion. The associated energy gain is the driving force for the scroll-to-nanotube conversion.

In order to determine possible activation barriers that would hinder the zipper motion, we calculated the energy associated with the concerted bond rearrangement, involving an sp^2/sp^3 rehybridization, using the atomistic approach. The total energy per layer in an infinite stack of graphitic layers is displayed in Fig. 3(e) as a function of the axial position z of the dislocation, where $z < 0$ corresponds to a defect-free graphitic structure. In structures with a finite number of layers, the z dependence of $\partial E_{tot}/N_L$ at $z > 0$ acquires an additional gradient due to the average energy gain per layer associated with the elimination of exposed edges.

Our results in Fig. 3(e) indicate that the activation barrier associated with axially displacing the dislocation region by one unit cell is surprisingly small, namely only ≤ 0.02 eV. In scrolls with N_L layers and exposed edges, this activation barrier is further reduced due to the gradient of $\partial(E_{tot}(z)/N_L)/\partial z$. In systems with less than hundred walls, the gradient is sufficiently large to make the scroll-to-tube conversion activation free. Since the activation barrier is so small in any multiwall system, we expect the zipperlike scroll-to-tube transformation to occur efficiently even at room temperature. Only much higher activation barriers, possibly associated with defects or impurities, could stop the scroll-to-tube conversion in a transition state.⁹

In conclusion, using total energy calculations, we investigated the relative stability of various sp^2 bonded structures, including graphitic scrolls and multiwall nanotubes. Our structure optimization studies have shown that a tubular shape with many walls is favored for very large systems. When grown in absence of catalysts, such structures should share similar interior diameters of ≈ 1.8 nm, in agreement with electron microscopy observations. We found that segments of nested multiwall nanotubes may coexist with scrolls within the same tubular nanostructure, separated by a dislocation region. The low energy cost to create this defect suggests that hybrid multiwall structures should likely form under common synthesis conditions. We proposed a concerted bond-rearrangement mechanism that would displace the dislocation axially, like a zipper, thus converting the less stable scroll into a multiwall nanotube. Due to the low energy cost of the bond rearrangement, we find that the scroll-to-nanotube conversion may proceed even at room temperature. We expect the nested walls in multiwall nanotubes, which originate from transformed scrolls, to share the same chirality.

This work has been partly supported by NSF-NIRT Grant No. DMR-0103587.

¹S. Iijima, *Nature (London)* **354**, 56 (1991).

²M. S. Dresselhaus, G. Dresselhaus, and P. C. Eklund, *Science of Fullerenes and Carbon Nanotubes* (Academic, San Diego, 1996), and references therein.

³J. W. Mintmire, B. I. Dunlap, and C. T. White, *Phys. Rev. Lett.* **68**, 631 (1992).

⁴R. Saito, M. Fujita, G. Dresselhaus, and M. S. Dresselhaus, *Appl. Phys. Lett.* **60**, 2204 (1992).

⁵N. Hamada, S. Sawada, and A. Oshiyama, *Phys. Rev. Lett.* **68**, 1579 (1992).

⁶X. F. Zhang, X. B. Zhang, G. Van Tendeloo, S. Amelinckx, M. Op de Beeck, and J. Van Landuyt, *J. Cryst. Growth* **130**, 368 (1993).

⁷O. Zhou, R. M. Fleming, D. W. Murphy, C. H. Chen, R. C. Haddon, A. P. Ramirez, and S. H. Glarum, *Science* **263**, 1744 (1994).

⁸S. Q. Feng, D. P. Yu, G. Hub, X. F. Zhang, and Z. Zhang, *J. Phys. Chem. Solids* **58**, 1887 (1997).

⁹J. G. Lavin, S. Subramoney, R. S. Ruoff, S. Berber, and D. Tománek, *Carbon* **40**, 1123 (2002).

¹⁰D. Tománek, W. Zhong, and E. Krastev, *Phys. Rev. B* **48**, 15 461 (1993).

¹¹D. H. Robertson, D. W. Brenner, and J. W. Mintmire, *Phys. Rev.*

B **45**, 12 592 (1992).

¹²We note that the contact area $A_c = A - \pi(R_{in} + R_{out})L$ is smaller than the total area A , since the innermost and outermost walls with the respective radii R_{in} and R_{out} have only one neighboring layer.

¹³V. P. Dravid, X. Lin, Y. Wang, X. K. Wang, A. Yee, J. B. Ketterson, and R. H. P. Chang, *Science* **259**, 1601 (1993).

¹⁴D. Tománek and M. A. Schluter, *Phys. Rev. Lett.* **67**, 2331 (1991).

¹⁵Y.-K. Kwon, Y. H. Lee, S. G. Kim, P. Jund, D. Tománek, and R. E. Smalley, *Phys. Rev. Lett.* **79**, 2065 (1997).

¹⁶K. Umamoto, S. Saito, S. Berber, and D. Tománek, *Phys. Rev. B* **64**, 193409 (2001).

¹⁷To avoid edge effects, we used periodic boundary conditions and finite unit cells. Constraints, imposed by the boundary conditions, increase the apparent dislocation energy for small unit cell sizes. In our calculations, we enlarged the unit cell size beyond that depicted in Fig. 3(d), until reaching convergence for the structure within the dislocation region and the value of the dislocation energy. Our results agree with *ab initio* results for moderate unit cell sizes, which are accessible to first-principles calculations.